IOPscience iopscience.iop.org

Home Search Collections Journals About Contact us My IOPscience

A Raman spectroscopic and energy-dispersive X-ray diffraction study of the high-pressure phase transitions of sodium hydrogen fluoride

This article has been downloaded from IOPscience. Please scroll down to see the full text article.

1992 J. Phys.: Condens. Matter 4 8131

(http://iopscience.iop.org/0953-8984/4/41/008)

View the table of contents for this issue, or go to the journal homepage for more

Download details:
IP Address: 171.66.16.96
The article was downloaded on 11/05/2010 at 00:40

Please note that terms and conditions apply.

J. Phys.: Condens. Matter 4 (1992) 8131–8140. Printed in the UK

A Raman spectroscopic and energy-dispersive x-ray diffraction study of the high-pressure phase transitions of sodium hydrogen fluoride

Andrew G Christy†, Julian Haines† and Simon M Clark‡

† Department of Chemistry, University of Leicester, Leicester LE1 7RH, UK
‡ Daresbury Laboratory, Daresbury, Cheshire WA4 4AD, UK

Received 22 May 1992

Abstract. Under ambient conditions, $NaHF_2$ adopts a rhombohedral structure ($R\bar{3}m$, $Z = 3$, $a = 3.474(1)$ Å, $c = 13.788(10)$ Å, $Z = 3$). Two high-pressure phase transitions have been noted previously, which we have located at 5 kbar and 41 kbar. We have studied all three phases by Raman spectroscopy and energy-dispersive x-ray diffraction. The symmetric [FHF] stretching vibration is at a significantly higher frequency in phase I (631 cm^{-1} at ambient) than in phase II (623 cm^{-1} and 612 cm^{-1} at 10.6 kbar). The phase I structure is also incompressible down the triad axis, along which the [FHF] groups are oriented. The implication is that the [FHF] anions act as rigid braces in the phase I structure.

The phase II x-ray data were fitted by a monoclinically distorted marcasite-like cell ($P2/m$, $a = 4.825(12)$ Å, $b = 3.188(13)$ Å, $c = 5.128(25)$ Å, $\beta = 91.16(29)°$, $Z = 2$ at 27.0 kbar). This structure is easily derived from that of phase I by a shear, with accompanying rotation of the [FHF] groups into two distinct orientations, consistent with the observed splitting of the Raman modes. Although displacive, the transformation is first order, with a 13.3% volume reduction at the transition pressure.

A further 5% volume discontinuity occurs at the II–III transition. The diffraction data for phase III index on a tetragonal cell whose dimensions suggest a variant of the structure adopted by KHF_2 at ambient pressure ($P4/ncc$, $a = 7.193(6)$ Å, $c = 5.657(22)$ Å, $Z = 8$ at 41.6 kbar). The [FHF] groups are canted in four or eight different directions. Simple diffusionless transformation pathways between the proposed phase II and phase III structures are suggested.

1. Introduction

The linear anions $[FHF]^-$ and $[NNN]^-$ form salts with the heavier alkali metals and Tl^+ whose structures under ambient conditions are simple tetragonally or trigonally distorted variants of the cubic NaCl and CsCl structure types [1]. We have found elsewhere [2] that when there is a polarizable or intrinsically non-spherical species present, the structures adopted with increasing pressure and coordination number are not necessarily analogues of the B3 (four-coordinated)–B1 (six-coordinated)–B2 (eight-coordinated) progression. Even when the principal cation–anion bonds are highly ionic, the increased relative importance of other interactions at pressure results in the stabilization of structural topologies that are unusual at atmospheric pressure, such as the TlI type in the case of the alkali hydroxides and hydrosulphides [2, 3].

0953-8984/92/418131+10$04.50 © 1992 IOP Publishing Ltd

High-pressure transitions of $NaHF_2$ to new phases had previously been identified at 4–8.5 kbar [4, 5] and near 40 kbar [6], but the structures of the new phases remained unknown. Therefore, this compound was selected for study, as an example of a system in which linear, symmetrical anionic groups are present. We have obtained Raman spectra for $NaHF_2$ up to 95 kbar, and x-ray diffraction data up to 65 kbar in diamond anvil cells. The diffraction data for both high-pressure phases were indexed, giving unit cells which suggested specific structural models for the phases, and straightforward diffusionless transformation paths between them.

2. Experimental procedure

The $NaHF_2$ used in this study was obtained commercially (BDH, 98% minimum assay). For Raman study, the sample was loaded into a diamond anvil cell under a N_2 atmosphere, with ruby chips for pressure calibration. A 450 μm thick prestressed stainless steel gasket was used, with a sample hole of $\simeq$ 250 μm diameter. Data were collected on a Coderg T-800 spectrometer, using the 488.0 nm line of a Spectra Physics 164 argon-ion laser. Peak positions were measured manually, to the nearest 0.25 cm^{-1} for sharp peaks. In general, estimated errors were ± 1 cm^{-1} (0–20 kbar), ± 2 cm^{-1} (20–40 kbar) and ± 3 cm^{-1} (> 40 kbar).

For x-ray study, the sample was ground in an agate mortar and pestle with NaCl as an internal pressure calibrant. The sample + calibrant mixture was then placed in the cell ($\simeq$ 100 μm diameter gasket hole) with Nujol as the quasihydrostatic pressure medium. This was done in air, since the sample did not hydrolyse rapidly in the dry, air-conditioned environment of the experimental station. Energy-dispersive x-ray spectra were collected on station 9.7 at Daresbury Laboratory, each run being about 20 minutes in duration. The diffraction angle used was about 7°. Subsequently, diffraction peaks were measured using the NGAUS fitting routine on the station μVAX. The initial indexing was done manually. Confirmations of indexing and cell refinement were performed using the routines REFCEL and DRAGON on the Daresbury Convex.

3. Results

Raman spectra for $NaHF_2$ at five different pressures are shown in figure 1, and the pressure variation of the Raman modes in figure 2. Frequency and pressure-derivative data are given in numerical form in table 1. For phase I, with factor group $R\bar{3}m$ and primitive unit cell content $Z' = 1$, there are only two Raman-active [FHF] fundamentals, an e_g libration at 145 cm^{-1} (at 1 bar) and an a_{1g} symmetrical stretch at 631 cm^{-1}. Notice that the symmetric [FHF] stretch decreases abruptly on going from phase I to phase II, and also splits into two bands, indicating that $Z' \geqslant 2$ for phase II, and that the F–H–F bonding is somewhat weaker than in phase I (see below). The Raman data put the I–II transition at 5 ± 1 kbar and the II–III transition at 41 ± 2 kbar. The former figure compares closely with the pressure of 3.85 ± 0.3 kbar determined by Pistorius and Campbell White at 19.8 °C [5].

Dawson *et al* [7] published assigned Raman and infrared spectra for KHF_2 under ambient conditions. By analogy with their data, a $NaHF_2$ phase of related structure should have two Raman-active librational modes at frequencies considerably above 100 cm^{-1} and 140 cm^{-1} respectively, and two symmetric [FHF] stretching modes

Table 1. Raman modes and pressure dependencies for the $NaHF_2$ phases. Intensities: S = strong, M = medium, W = weak. ν_0 = wavenumber at zero pressure, extrapolated along the linear regression line, with RMS deviation of the data from the fitted line. The estimated SD for the pressure derivative is

$$\sqrt{\left(\sum(\nu_{obs} - \nu_{regr})^2/(N-2)\sum(P_{obs} - \overline{P})^2\right)}$$

where N = number of data points per dataset.

ν (cm^{-1})	ν_0 (cm^{-1})	$\partial\nu/\partial P$ (cm^{-1} $kbar^{-1}$)
Phase I (0 kbar)		
631 S	630.3(3)	0.83(5)
145 M	144.5(7)	0.65(13)
Phase II (10.6 kbar)		
623 W	619.3(14)	0.47(3)
612 M	607.8(7)	0.42(2)
190 W	178.4(3)	1.07(26)
150 M	144.1(20)	0.58(7)
Phase III (57.1 kbar)		
656 M	627.6(29)	0.48(8)
627 M	612.5(16)	0.27(4)
184 M	137.3(11)	0.81(4)
159 W	153.1(9)	0.13(5)

at 600–700 cm^{-1}. Note that this is the case for the spectra of both phase II and phase III, although there may be further splitting for phase III since the values of ν_0 suggest that both modes observed may correlate with the 143–150 cm^{-1} modes of phases I and II. It is not surprising that Whalley [8] commented on the spectroscopic similarity between phase II and KHF_2, although the diffraction data of Bradley *et al* [4] cannot be fitted on a KHF_2-like cell. Hamann and Linton [6] did not see a resemblance between the infrared spectra of phase III and that of KHF_2; this appears to be because their sample was intergrown with phase II, as they suggest.

Energy dispersive x-ray diffraction patterns for the three phases are shown in figure 3, refined cell parameters in figure 4, and volumes per formula unit in figure 5. There is considerable overlap in the pressure domain between datasets for different phases, since phase I persisted up to 18 kbar on compression, and phase III down to 33 kbar on decompression. Cell data and compressibilities are also presented in table 2. The extreme anisotropy of compressibility for phase I is noteworthy: the [FHF] groups evidently act as rigid braces along the z axis, all compression occurring in the xy plane. The lack of free rotation of the [FHF] groups presumably places them under considerable compression, accounting for the highly symmetric stretching frequency and large positive value of $\partial\nu/\partial P$ in this phase relative to phases II and III.

Observed and calculated d-spacings for phases II and III are shown in table 3.

The unit cell determined for phase II bears no relation to that proposed by Bradley *et al* [4], although it is consistent with all their observed x-ray lines. Our cell was obtained after calculating peak positions for hypothetical $NaHF_2$ polymorphs with other known structures containing linear ions. The orthorhombic marcasite structure, cell parameters estimated from assumed Na–F and F–H–F bond lengths, was found to give a good fit to the observed peak positions. The fit improved on making the two longer axes of the cell non-orthogonal (β = 91.0–91.8°). Therefore, we propose that

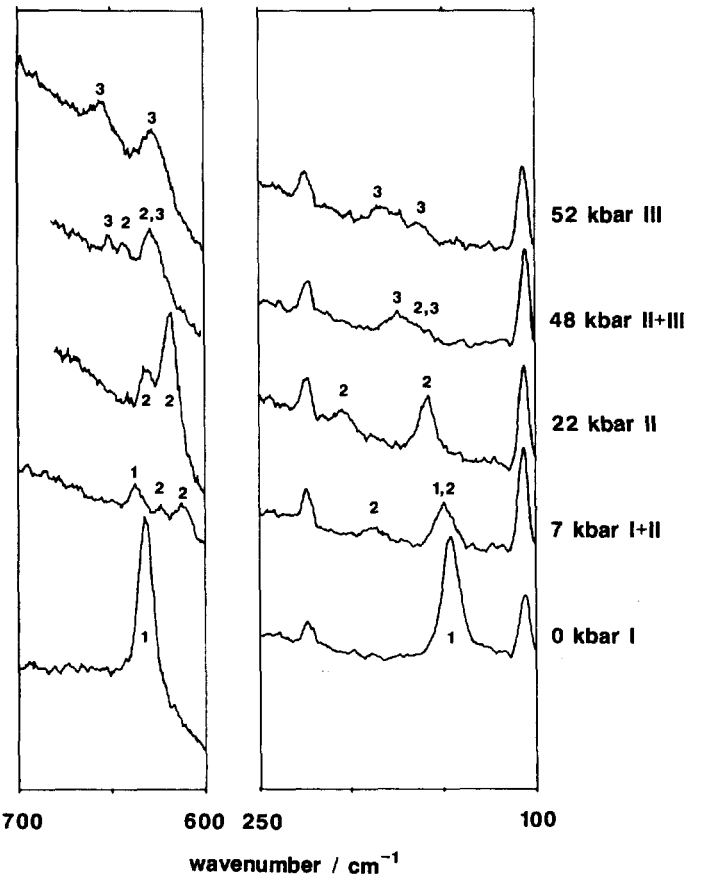

Figure 1. Raman spectra for $NaHF_2$ over the ranges 600–700 cm^{-1} and 100–250 cm^{-1}. Peaks at 106 and 224 cm^{-1} are laser lines. '1', '2' and '3' indicate peaks from phases I, II and III respectively.

the cell is monoclinic, $P2/m$, $Z = 2$. The compressibility is very low along the z direction in this structure as well; presumably, the [FHF] groups rotate more readily toward this direction than away from it on compression. Our volume change at the I–II transition pressure is from 47.1 to 40.8 Å^3/molecule to (−13.3%), more than twice that calculated by Pistorius and Campbell White [5] from their piston cylinder displacement measurements. It is possible that they did not estimate the start and end points of this rather sluggish transition correctly.

Phase III gave relatively few diffraction peaks, and was indexed on a tetragonal cell by inspection. The cell constants were close to those expected for a KHF_2-like phase of $NaHF_2$ (cf Pistorius and Campbell White's estimated volume of 35 Å^3/molecule for such a phase, compared with our volume of 38.4 Å^3 extrapolated back to room pressure). However, the presence of superlattice peaks implied that the true x and y axes were in fact at 45° to those of KHF_2, and that the unit cell content was double that of the potassium salt. The only simple displacement that was found to give this cell doubling while retaining $4/mmm$ point symmetry was a rotation of the [FHF] groups out of the xy plane, in the space group $P4/ncc$ (rotation about z is also

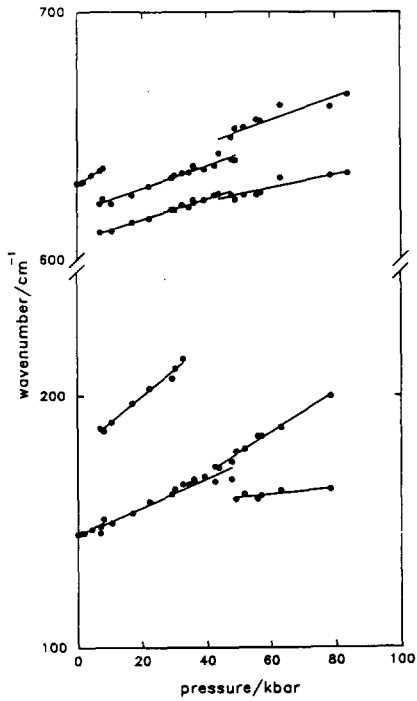

Figure 2. Raman modes versus pressure for $NaHF_2$-I, II and III.

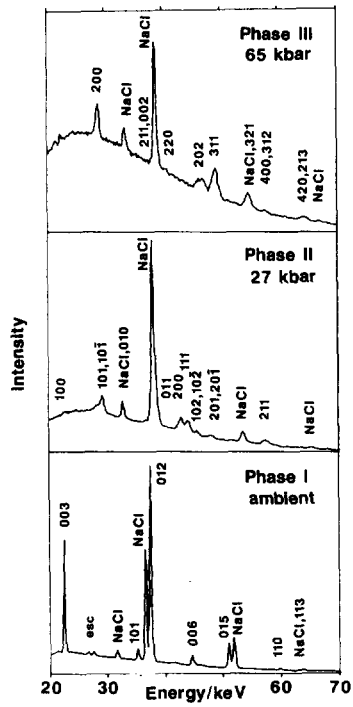

Figure 3. Energy-dispersive x-ray diffraction patterns for $NaHF_2$-I, II and III. Peaks indicated by 'esc' are escape peaks.

permitted since the [FHF] ions no longer lie along diads in this space group). The structure of phase III is therefore a linear-ion derivative of the CsCl structure with [FHF] groups oriented in at least four if not eight different directions.

4. Discussion

If the $R\bar{3}m$ structure of phase I and the $P2/m$ structure of phase II are viewed down diad axes, a close structural relationship is apparent. $(10\bar{1}2)$ structural slabs of the phase I structure consist of rectangular nets of Na atoms, centred by [FHF] groups, all of which are similarly canted at 66° to the plane normal. Reversal of the canting direction in alternate slabs, accompanied by an overall monoclinic shear, gives the phase II structure, as can be seen from the ORTEP plots of figure 6. Geometrically, the relationship between rhombohedral and the ideal marcasite structures is one of 'unit cell twinning' (cf the relationship between ortho- and clino-pyroxene and amphibole structures [9]). The actual symmetry of phase II is a subgroup common to both higher-symmetry structures. The relationship suggests that the transition is driven by collapse at the Brillouin zone boundary (F point, [10]) of a lattice mode dominated by [FHF] libration in the xz plane. Thus, a possible solution is found to the puzzle posed by Pistorius and Campbell White [5] in the discussion section of their paper. They ask why no $NaHF_2$ analogue has been found for phase II in the NaN_3 system. NaN_3-II is monoclinic, $C2/m$, and the $R\bar{3}m$–$C2/m$ transition is close to second

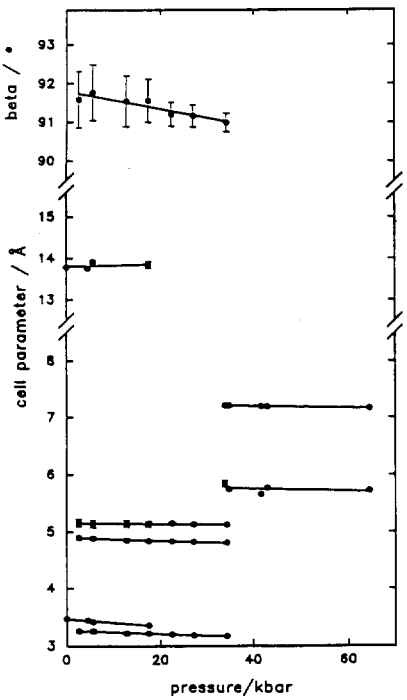

Figure 4. Variation of cell parameters with pressure for $NaHF_2$-I, II and III.

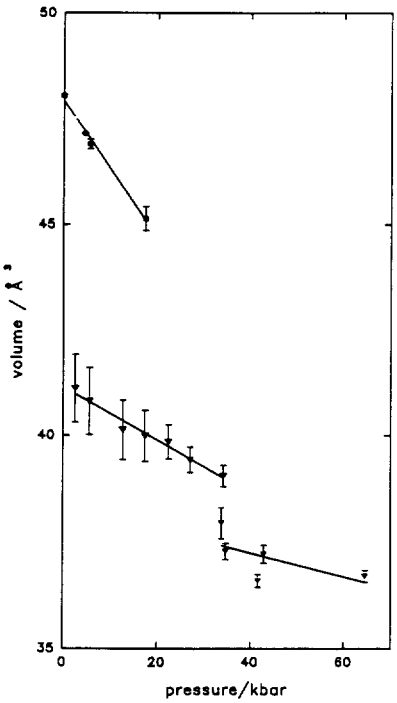

Figure 5. Volume per formula unit versus pressure for $NaHF_2$ phases.

Table 2. Cell parameters and pressure derivatives for the $NaHF_2$ phases. Cell parameter estimated errors are for fits to individual diffraction datasets at specified pressures. V is the volume per formula unit. 'Compressibilities' are $-1000(1/a)(\partial a/\partial P)$ etc, expressed in units of $kbar^{-1}$. Derived from linear regression of refined cell data. The estimated standard deviations were calculated as for the pressure derivatives in table 1.

	Phase I (0 kbar)	Phase II (27.0 kbar)	Phase III (41.6 kbar)
Space group:	$R\bar{3}m$	$P2/m$	$P4/ncc$
a (Å)	3.474(1)	4.825(12)	7.193(6)
b (Å)		3.188(13)	
c (Å)	13.788(10)	5.128((25)	5.657(22)
β (deg)		91.16(29)	
Z	3	2	8
V (Å^3)	48.04(4)	39.43(30)	36.59(15)
Compressibilities			
a	1.83(28)	0.54(6)	0.20(2)
b		0.88(16)	
c	−0.21(44)	0.12(6)	0.34(50)
β		0.25(4)	
V	3.41(59)	1.52(18)	0.73(50)

order [11] although permitted third-order terms in the Landau free energy imply that the transition is discontinuous [12]. This transition is clearly associated with softening of the phase I e_g mode at the zone centre, losing the triad axes but retaining all

Table 3. Calculated and observed d-spacings for $NaHF_2$-II and $NaHF_2$-III.

hkl	d_{obs}	d_{calc}	$100(d_{obs} - d_{calc})/d_{calc}$
Phase II (27.0 kbar)			
100	4.771	4.824	−1.1
$10\bar{1}$, 101	3.554	3.513	+1.2
010	3.165	3.188	−0.7
011	2.705	2.707	−0.1
200	2.419	2.412	+0.2
$11\bar{1}$		2.372	(+0.7)
111	2.356	2.350	−0.3
$10\bar{2}$, 102	2.282	2.264	+0.8
$20\bar{1}$, 201	2.160	2.183	−1.1
$21\bar{1}$	1.806	1.811	−0.3
211		1.791	(+1.4)
Phase III (41.6 kbar)			
200	3.592	3.597	−0.1
002		2.829	(−0.9)
211	2.803	2.796	+0.3
220	2.548	2.543	+0.2
202	2.214	2.223	−0.4
311	2.108	2.111	−0.1
321	1.889	1.881	+0.4
400	1.797	1.798	−0.1
312		1.773	(+1.4)
213		1.627	(−1.4)
420	1.605	1.608	−0.2

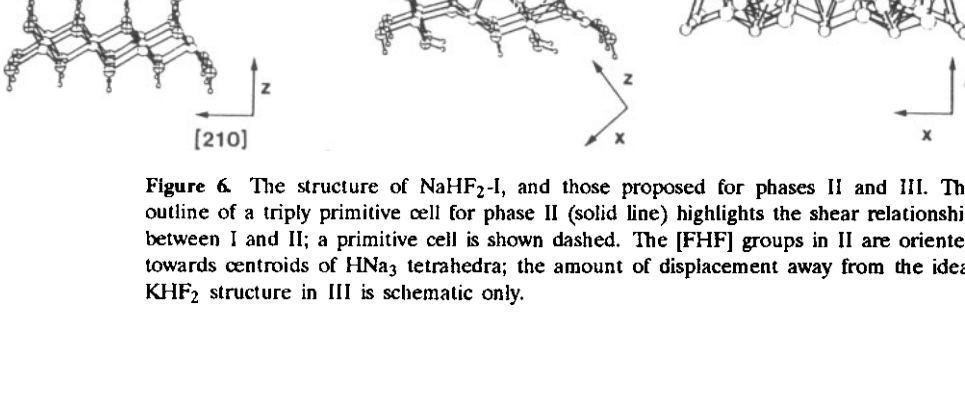

Figure 6. The structure of $NaHF_2$-I, and those proposed for phases II and III. Th outline of a triply primitive cell for phase II (solid line) highlights the shear relationshi between I and II; a primitive cell is shown dashed. The [FHF] groups in II are oriente towards centroids of HNa_3 tetrahedra; the amount of displacement away from the ide KHF_2 structure in III is schematic only.

translational symmetry. The mode associated with the phase I–phase II transition in $NaHF_2$ is a zone *boundary* correlative of the same. The rotations of neighbouring [FHF] groups about y alternate in sense rather than being all the same. Additionally, there is clearly a strong potential minimum associated with approximation of the higher-symmetry marcasite structure. Therefore, the $NaHF_2$ transition is markedly discontinuous. Otherwise, the I–II transitions in $NaHF_2$ and NaN_3 are similar.

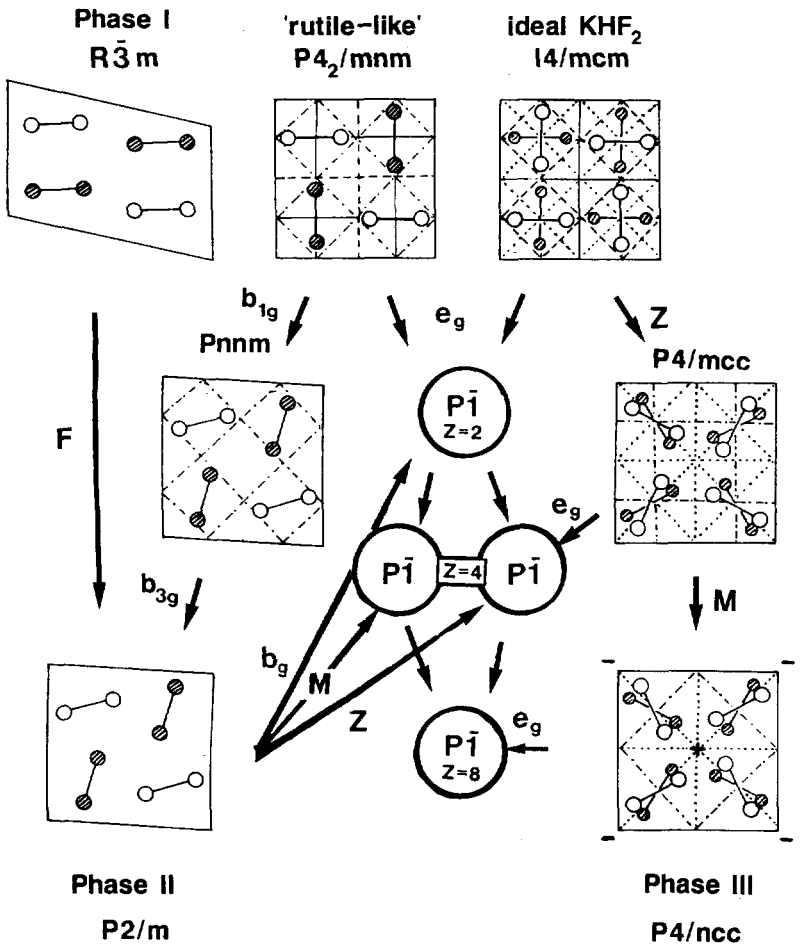

Figure 7. Possible diffusionless transformation paths between phases I, II, and III. Orientation is shown by indication of vertical mirror and glide planes. Shading of F atoms indicates half lattice repeat height out of the page. The symbols '+' and '–' indicate elevation slightly above or below this value for a group of F atoms.

Given the simple relationship between the phase I and phase II structures, it is not surprising that both structures in figure 6 can be regarded as NaCl-like arrays distorted by the elongated shape of the anion, viewed down $[110]_{NaCl}$ in both cases. It is interesting to note that the other polymorph of FeS_2, pyrite, has a structure that is also derived from the rocksalt structure by replacing spherical anions with $[S_2]$ dumbells. Pyrite retains cubic symmetry (space group $Pa3$) and is slightly denser

than marcasite. The pyrite form of FeS_2 is stable to above 300 kbar [14], and one can speculate a bifluoride analogue of pyrite might have become stable at pressure if the phase III structure had not been adopted first. Interpolation of H atoms at the centre of the F–F dumbells would have provided an interesting intermediate case between the structures of SiP_2 (isostructural with pyrite) and SiP_2O_7 (similar but with additional O inserted into all Si–P and P–P linkages).

Another structure closely related to those of marcasite and $NaHF_2$-II is that of rutile (TiO_2), adopted by many dioxides and difluorides of six-coordinated cations. The $Pnnm$ marcasite structure differs from that of rutile ($P4_2/mnn$) only in the existence of di-anion bridges and an accompanying orthorhombic distortion (note the subgroup–supergroup relationship between symmetries). There is considerable similarity also between such a rutile-like structure and the low-pressure structure of KHF_2. These two structures may be interconverted by a shearing operation, with e_g as the active irreducible representation of both tetragonal phases. On the basis of this geometrical relationship, it is possible by dropping into the appropriate subgroup symmetries to derive diffusionless pathways between $NaHF_2$-II and $NaHF_2$-III via a minimum of two intermediate transition structures. These are the possible transformation mechanisms between observed phases that involve the minimum number of concerted atomic displacements, although they are not necessarily those actually adopted. These relationships are shown in figure 7. The orientations of [FHF] groups are shown for corresponding quadruply primitive cells of all structures with monoclinic or higher symmetry. Each structure is labelled with its space group, and each potentially continuous transformation path by the active irreducible representation of the higher-symmetry structure. If the transformation is at the zone boundary, the irrep is identified by the appropriate reciprocal space symmetry point only: F = cell doubling along y^* (rhombohedral lattice, hexagonal axial setting), Z = doubling along z^*, M = doubling along x^*+y^*. It is emphasized that the paths shown in figure 6 are not exhaustive, but are the shortest out of an infinitude of possibilities. Although hypothetical for $NaHF_2$ at present, multistage diffusionless transformation paths like these ones are likely to be important solid-state transformation mechanisms, particularly at high pressure, where short interatomic distances and strong repulsions present considerable obstacles to diffusion of atoms. There is some experimental evidence for the existence of such transformation paths in the PbO system [13].

Acknowledgments

This study was supported by the SERC of Great Britain (AGC) and NSERC of Canada (JH). We would like to thank David M Adams for the use of his laboratory and stimulating discussions during the development of this work, and also two anonymous reviewers whose comments improved this paper.

References

[1] Wyckoff R W G 1964 *Crystal Structures* vol 2 (New York: Interscience)
[2] Haines J and Christy A G 1992 *Phys. Rev.* B **46** in press
[3] Adams D M, Christy A G and Haines J 1992 *J. Phys. C: Solid State Phys.* in press
[4] Bradley R S, Grace J B and Munro D C 1964 *Z. Kristallogr.* **120** 349
[5] Pistorius C W F T and Campbell White A J 1970 *High Temp.–High Pressures* **2** 507

[6] Hamann S D and Linton M 1976 *Aust. J. Chem.* **29** 479
[7] Dawson P, Hargreave M M and Wilkinson G R 1975 *Spectrochim. Acta* A **31** 1055
[8] Whalley E 1974 *Proc. 4th Int. Conf. High Pressure (Kyoto, 1974)* p 35
[9] Ito T 1950 *X-ray studies on Polymorphism* (Tokyo: Maruzen)
[10] Bradley C J and Cracknell A P 1972 *The Mathematical Theory of Symmetry in Solids* (Oxford: Clarendon)
[11] Pringle G and Noakes D 1968 *Acta Crystallogr.* B **24** 262
[12] Tolédano J-C and Tolédano P 1980 *Phys. Rev.* B **21** 1139
[13] Adams D M, Christy A G, Haines J and Clark S M 1992 *Phys. Rev.* B **46** in press
[14] Chattopadhyay T 1992 personal communication